Advances in Water Resources 87 (2016) 29–41

Contents lists available at ScienceDirect

Advances in Water Resources

journal homepage: www.elsevier.com/locate/advwatres

Inter- and intra-annual variation of water footprint of crops and blue water scarcity in the Yellow River basin (1961–2009)

La Zhuo [a,*], Mesfin M. Mekonnen [a], Arjen Y. Hoekstra [a], Yoshihide Wada [b]

[a] Twente Water Center, University of Twente, P. O. Box 217, 7500AE Enschede, The Netherlands
[b] Department of Physical Geography, Utrecht University, 3508TC Utrecht, The Netherlands

ARTICLE INFO

Article history:
Received 15 May 2015
Revised 29 October 2015
Accepted 3 November 2015
Available online 10 November 2015

Keywords:
Yellow River Basin
Maximum sustainable water footprint
Blue water scarcity
Crop production
Inter- and intra-annual assessment

ABSTRACT

The Yellow River Basin (YRB), the second largest river basin of China, has experienced a booming agriculture over the past decades. But data on variability of and trends in water consumption, pollution and scarcity in the YRB are lacking. We estimate, for the first time, the inter- and intra-annual water footprint (WF) of crop production in the YRB for the period 1961–2009 and the variation of monthly scarcity of blue water (ground and surface water) for 1978–2009, by comparing the blue WF of agriculture, industry and households in the basin to the maximum sustainable level. Results show that the average overall green (from rainfall) and blue (from irrigation) WFs of crops in the period 2001–2009 were 14% and 37% larger, respectively, than in the period 1961–1970. The annual nitrogen- and phosphorus-related grey WFs (water required to assimilate pollutants) of crop production grew by factors of 24 and 36, respectively. The green–blue WF per ton of crop reduced significantly due to improved crop yields, while the grey WF increased because of the growing application of fertilizers. The ratio of blue to green WF increased during the study period resulting from the expansion of irrigated agriculture. In the period 1978–2009, the annual total blue WFs related to agriculture, industry and households varied between 19% and 52% of the basin's natural runoff. The blue WF in the YRB generally peaks around May–July, two months earlier than natural peak runoff. On average, the YRB faced moderate to severe blue water scarcity during seven months (January–July) per year. Even in the wettest month in a wet year, about half of the area of the YRB still suffered severe blue water scarcity, especially in the basin's northern part.

1. Introduction

The increasing demand for fresh water by humanity is challenging the sustainable water use in many river basins around the world [30,67,69]. The Yellow River Basin (YRB, or "Huang He"), the second largest river basin of China, with a drainage area of 795×10^3 km^2 [76], is well known as one of the world's basins facing severe water scarcity. The YRB is now responsible for producing 13% of national grain production with only 2% of the national water resources [76]. In the last half century, with a booming agriculture and burgeoning population, the total consumption of blue water (ground and surface water) by agriculture, industry and households in the YRB increased from 17.8×10^9 m^3 in the 1960s [11] to 39.3×10^9 m^3 in 2009 [75]. Agriculture is by far the largest water user in the basin, accounting for 77% of the total blue water consumption, of which 91% is used for field irrigation (2009) [75]. In 2009, the total annual water withdrawal in the YRB for agriculture, industry and households reached 76.5% of the renewable water resources in the basin [75]. In recent years, competition among the different sectors over the limited water resources has intensified [78]. Meanwhile, when comparing the 1960s to 2000s, precipitation and evaporation showed downward trends in most areas within the YRB [40,72]. The yearly natural runoff of the YRB decreased constantly in the 1990s [71] and reached its lowest value in 2002 ($\sim30.0\times10^9$ m^3), after which it increased again and remained fluctuating (at an average level of $\sim57.5\times10^9$ m^3) [75]. As a result of climatic variability, the inter-annual variability of natural water availability and water demand in the YRB are large, whereby demand in agriculture is typically high when availability is low.

Unfortunately, data on variability of and trends in water consumption, pollution and scarcity in the YRB are lacking. Another problem is that traditional statistics like 'annual gross water abstraction' per sector and 'irrigation efficiency' in the agricultural sector do not provide a comprehensive picture of water use and water scarcity. For understanding water scarcity at catchment or river basin level, we need to measure net water abstraction (consumptive water use) rather than gross water abstraction, because return flows can be reused and thus do not contribute to water scarcity [29]. A similar shortcoming exists with the indicator of irrigation efficiency, which measures

* Corresponding author. Tel.: +31 534892585.
E-mail address: l.zhuo@utwente.nl, zhuo.l@hotmail.com (L. Zhuo).

http://dx.doi.org/10.1016/j.advwatres.2015.11.002
0309-1708/

losses between gross water abstraction and the volume of water that reaches the crop. Only a part of this so-called loss, namely the part that evaporates, is really lost to the catchment and will thus contribute to scarcity; a large part of the so-called loss refers to water that percolates and thus adds to the groundwater and remains available in the catchment [47]. Another gap in traditional statistics is the focus on the use of blue water resources (ground and surface water), which is insufficient, given the fact that agriculture heavily relies on green water resources (rainwater) [17]. Besides, water pollution and water scarcity are intricately linked, because the effect of pollutants becomes worse if groundwater and river flows get depleted. Finally, usual statistics on water use and scarcity are annual, while the key to understanding water use and scarcity is the recognition of intra-annual variability [55]. The water footprint (WF) – introduced by Hoekstra [27] – is a comprehensive measure of human freshwater appropriation that addresses these shortcomings.

The WF is a multi-dimensional indicator that measures consumptive water use of both rainfall and ground-surface water (the green and blue WF, respectively) and the water required to assimilate anthropogenic loads of pollutants to freshwater bodies (the grey WF) [29]. In geographic applications, several soil-water-balance models have been applied in order to map WFs at high spatial resolution levels so that one can see where they are located [25,38,41,54,57]. Rost et al. [54] estimated, using the LPJmL model at 30 arc min resolution level, total green and blue WFs in global crop production for 1971–2000. Hanasaki et al. [25] evaluated, employing the H08 model at 30 arc min resolution level, global total green and blue WFs of major crops for 1985–1999. Liu and Yang [38] estimated, based on the GEPIC model at 30 arc min resolution level, global total green and blue WFs of crop production for the year 2000. Siebert and Doll [57] computed, with the GCWM model at 5 arc min resolution level, global total green and blue WFs of major crops worldwide for 1998–2002. Mekonnen and Hoekstra [41] estimated, applying the Cropwat model at 5 arc min resolution level, the green, blue and grey WFs of crop production worldwide for 1996–2005. Cai et al. [10] and Feng et al. [22] applied an input–output model to evaluate the WF and regional virtual water trade for the YRB from a consumptive perspective for 2002 and 2007, respectively. Hoekstra et al. [30] estimated blue water scarcity for the major river basins in the world over the period 1996–2005, by taking, per basin, the ratio of blue WF to the maximum sustainable blue WF. Mekonnen and Hoekstra [43] estimated, at 5 arc min grid level, the global grey WF related to nitrogen for the period of 2002–2010. These studies show that the blue WF in the YRB is relatively large during several months per year [25,30,54,57] and has the highest blue water proportion in total consumptive (green + blue) use among river basins around the world [38]. Meanwhile, there is net virtual water export from the YRB [10,22]. The YRB faces severe blue water scarcity for four months per year, as a long-term average, mostly in spring time when runoff is still low while water consumption for irrigation starts to increase [30]. The nitrogen-related grey WF in the YRB has been estimated to be about eight times the annual runoff, which implies a very high water pollution level [43].

Although temporal and spatial variations in WFs are keys in understanding water scarcity, most existing geographic WF assessment studies consider one specific year or the average for a period of five to ten years. There are a few studies focusing on the long-term variability of green and blue WFs, for example, Zhuo et al. [80] and Tuninetti et al. [64] estimated WFs of four major crops in the YRB and globally, respectively, at 5 arc min grid level inter-annually over 1996–2005; Sun et al. [63] calculated WFs for grain production in the Hetao irrigation district over 1960–2008. But there are no water scarcity studies at a high temporal and spatial resolution for a series of years.

The current study aims at investigating (i) the temporal and spatial variability of green, blue and grey WFs of crop production in the YRB for the period of 1961–2009; and (ii) the temporal and spatial variability of blue water scarcity in the YRB for 1978–2009. The YRB is usually divided into three reaches: the upper reach (upstream of Hekouzhen, Inner Mongolia), the middle reach (upstream of Taohuayu, Henan Province) and the lower reach (draining into the Bohai Sea) [76]. This is the first river basin study that combines a high temporal resolution (WF estimated per day; blue water scarcity estimated per month), a high spatial resolution (5×5 arc min), and a multi-year record including both dry and wet years. In addition, the study is innovative in applying a combined soil-water-balance and crop-growth model in estimating the green and blue WFs in crop production. Most of earlier WF studies (e.g. [38,41,57,80]) applied a soil-water-balance model in combination with an assumed simple linear relationship between yield and evapotranspiration [16]. We applied, for the first time, the FAO crop water productivity model AquaCrop [31,49,61] to estimate crop WF. AquaCrop separately simulates crop transpiration (Tr) and soil evaporation (E) and the daily Tr is used to derive the daily biomass gain via the normalized biomass water productivity of the crop [61]. Compared to other crop growth models, AquaCrop has a significantly smaller number of parameters and better balances between simplicity, accuracy and robustness [60]. The model performance regarding crop water use and yield simulation has been widely tested for a number of crops under diverse environments and types of water management [1,3,21,24,34,35,62,77]. This is the first time that the AquaCrop model is applied to simulate crop water use and yields for a whole river basin, by running the model per crop for each grid cell. Besides, we added a module that separates green and blue water evapotranspiration in order to be able to calculate green and blue WFs of crops.

2. Method and data

2.1. Estimating green and blue water footprints in crop production

The WFs related to the production of seventeen major crops (listed in Table 1) in the YRB during the period 1961–2009 were estimated year by year with a daily time step at a 5×5 arc min grid (~7.4 km × 9.3 km at the latitude of the YRB) following the accounting framework of Hoekstra et al. [29]. The crops considered account for about 87% of the harvested area and 93% of crop production in 2009 [46]. Per crop, the green WF of producing a crop within a grid cell (in $m^3\ y^{-1}$) was estimated by multiplying the green water evapotranspiration (ET, $m^3\ ha^{-1}$) over the growing period by the harvested area for the crop (in ha y^{-1}). Similarly, the blue WF was estimated by multiplying the blue ET by the harvested area. The green or blue WF per unit of a crop (in $m^3\ t^{-1}$) was calculated per grid cell by dividing the green or blue ET over the growing period by the crop yield (Y, t ha^{-1}). The AquaCrop was used to simulate ET and Y for each type of crop per year per grid cell. Simulated Y per crop per year per grid cell was calibrated at provincial level, by scaling the model outputs in order to fit provincial crop yield statistics [46]. AquaCrop is a water-driven crop water productivity model with a dynamic daily soil water balance:

$$S_{[t]} = S_{[t-1]} + PR_{[t]} + IRR_{[t]} + CR_{[t]} - ET_{[t]} - RO_{[t]} - DP_{[t]} \quad (1)$$

where $S_{[t]}$ (mm) refers to the soil water content at the end of day t, $PR_{[t]}$ (mm) the precipitation on day t, $IRR_{[t]}$ (mm) the irrigation water applied on day t, $CR_{[t]}$ (mm) the capillary rise from groundwater, $ET_{[t]}$ (mm) actual evapotranspiration, $RO_{[t]}$ (mm) daily surface runoff and $DP_{[t]}$ (mm) deep percolation. $RO_{[t]}$ is estimated through the Soil Conservation Service curve-number equation [51]:

$$RO_{[t]} = \frac{\left(PR_{[t]} - 0.2 \times S\right)^2}{PR_{[t]} + S - 0.2 \times S} \quad (2)$$

where S (mm) refers to potential maximum storage, which is a function of the soil curve number. $DP_{[t]}$ is defined by the drainage ability ($m^3\ m^{-3}\ day^{-1}$) given the actual soil water content between

Table 1
Crop characteristics used in the current study.[a]

Crop	Planting date	Relative crop growing stages				HI_0	Max. rooting depth (m)	
		L_{ini}	L_{dev}	L_{mid}	L_{late}		Irrigated	Rain-fed
Winter wheat	15th October	0.48	0.22	0.22	0.07	40%	1.5	1.8
Spring wheat	15th March	0.15	0.19	0.44	0.22	39%	1	1.5
Rice	1st May	0.20	0.20	0.40	0.20	43%	0.5	1
Maize	1st May	0.20	0.27	0.33	0.20	44%	1	1.7
Sorghum	1st May	0.15	0.27	0.35	0.23	39%	1	2
Millet	15th April	0.14	0.21	0.39	0.25	38%	1	2
Barley	15th May	0.13	0.21	0.42	0.25	39%	1	1.5
Soybean	1st June	0.13	0.17	0.50	0.20	44%	0.6	1.3
Potato	1st May	0.19	0.23	0.35	0.23	59%	0.4	0.6
Sweet potato	1st May	0.13	0.20	0.40	0.27	69%	1	1.5
Cotton	1st April	0.17	0.28	0.31	0.25	38%	1	1.7
Sugar beet	15th April	0.28	0.22	0.28	0.22	71%	0.7	1.2
Groundnut	15th April	0.25	0.32	0.25	0.18	43%	0.5	1
Sunflower	15th April	0.19	0.27	0.35	0.19	31%	0.8	1.5
Rapeseed	15th March	0.20	0.40	0.20	0.20	25%	1	1.5
Tomato	15th January	0.22	0.30	0.30	0.19	40%	0.7	1.5
Apple	1st March	0.13	0.21	0.54	0.13	20%	0.7	1.5

[a] Sources: reference harvest indexes from Xie et al. [70] and Zhang and Zhu [79]; planting dates from Chen et al. [13]; relative crop growing stages and maximum rooting depths from Allen et al. [2] and Hoekstra and Chapagain [28].

saturation and field capacity. The drainage ability is zero when the soil water content is lower than or equal to field capacity [50].

By tracking daily incoming and outgoing water fluxes at the boundaries of the root zone we were able to separate the green and blue soil water balances at a daily basis. The $CR_{[t]}$ is assumed to be zero because the ground water depth is considered to be much larger than 1 m [2]. In order to obtain initial soil water content at the beginning of the growing period, following the method and assumption from [57], the initial soil water moisture was simulated from the maximum soil water content through two years rain-fed fallow land prior to the planting date. The initial soil water moisture at the start of the growing period is assumed as green water.

The contribution of precipitation (green water) and irrigation (blue water) to surface runoff is calculated based on the respective magnitudes of precipitation and irrigation to the total green plus blue water inflow. The green and blue components in DP and ET are calculated per day based on the fractions of green and blue water in the total soil water content at the end of the previous day. The green soil water content (S_{green}) and blue soil water content (S_{blue}) are thus calculated as:

$$\begin{cases} S_{green[t]} = S_{green[t-1]} + \left(PR_{[t]} + IRR_{[t]} - RO_{[t]}\right) \times \frac{PR_{[t]}}{\left(PR_{[t]}+IRR_{[t]}\right)} \\ \quad - \left(DP_{[t]} + ET_{[t]}\right) \times \frac{S_{green[t-1]}}{S_{[t-1]}} \\ S_{blue[t]} = S_{blue[t-1]} + \left(PR_{[t]} + IRR_{[t]} - RO_{[t]}\right) \times \frac{IRR_{[t]}}{\left(PR_{[t]}+IRR_{[t]}\right)} \\ \quad - \left(DP_{[t]} + ET_{[t]}\right) \times \frac{S_{blue[t-1]}}{S_{[t-1]}} \end{cases} \quad (3)$$

In AquaCrop, the daily crop transpiration ($Tr_{[t]}$, mm) is used to derive the daily gain in above-ground biomass (B) via the normalized biomass water productivity of the crop (WP^*, kg m^{-2}):

$$B = WP^* \times \sum \frac{Tr_{[t]}}{ET_{0[t]}} \quad (4)$$

$WP*$ is normalized for the carbon dioxide (CO_2) concentration of the bulk atmosphere, the evaporative demand of the atmosphere (ET_0) and crop classes (C3 or C4 crops). The normalization makes the model applicable to diverse locations and seasons [50]. The harvestable portion (the crop yield Y, t ha^{-1}) of B at the end of the growing period is determined as product of B and the harvest index (HI, %):

$$Y = HI \times B \quad (5)$$

HI is adjusted to water and temperature stress depending on the timing and extent of the stress by an adjustment factor (f_{HI}) from the reference harvest index (HI_0):

$$HI = f_{HI} \times HI_0 \quad (6)$$

Vanuytrecht et al. [66] examined the sensitivity of *Y* to inputs in the AquaCrop model, and found that simulated *Y* is particularly sensitive to the root and soil parameters. Therefore, before running AquaCrop, input parameters on crop calendar, maximum effective root depth and HI_0 for each crop were carefully selected from different sources for the current study (Table 1). Values of other crop parameters used in the study are taken from Raes et al. [50]. Several studies [1,4,33,35] have verified that the model performs at acceptable accuracy level in *Y* simulations and the accuracy level was relatively higher for irrigated crops than rain-fed crops. This is due to the fact that if the soil water content reaches below the threshold affecting the canopy senescence in the model, the simulated canopy will die resulting in an underestimated or even zero *Y* [35,50]. Therefore, in order to avoid such modeling failures at rain-fed fields, we set the initial soil moisture such that the soil water threshold for canopy senescence for each crop is met.

2.2. Estimating grey water footprints in crop production

The grey WF related to crop production refers to the volume of water needed to assimilate the fertilizers and pesticides applied to the field that reach groundwater through leaching or surface water through runoff or soil erosion [29]. In the current study, we consider the effect of nitrogen (N) and phosphorus (P), thus excluding the effect of other nutrients and fertilizers. At a 5×5 arc min grid and annual basis, we estimated the grey WF of crop production related to N and P from both mineral and manure fertilizers during the period 1961–2009. The grey WF per unit of crop (WF_{grey}, m^3 t^{-1}) was calculated following the formula [29]:

$$WF_{grey} = \frac{\alpha \times AR}{(c_{max} - c_{nat})} \times \frac{1}{Y} \quad (7)$$

where α represents the leaching-runoff fraction, AR (kg ha^{-1}) the application rate to the field (the sum of mineral and manure fertilizer), c_{max} (mg l^{-1}) the maximum acceptable concentration of the nutrient in the receiving water body, and c_{nat} the natural concentration of the nutrient in the receiving water body. We used values for c_{max} and c_{nat} from China's national surface water quality standard [44] and average values for α as suggested in Franke et al. [23]: 0.1 for N, 0.03 for P.

The mineral and manure fertilizer application rates by crop and per grid cell were estimated following [39]. For both artificial fertilizer and manure, the fertilizer consumption volumes are expressed in terms of N and P amounts. The fertilizer volume per crop per year per grid cell was calculated from the total annual national fertilizer consumption for the crop times the production share of the grid cell. The correlated AR in a grid cell was calculated by dividing the crop-specific fertilizer volume by the harvested area of the crop. The manure input for a nutrient was calculated by multiplying the livestock density with animal specific excretion rates for the nutrient and excretion collection rates. Five types of livestock were considered: cattle, goats, sheep, pigs and poultry. Excreta can be produced in either stables or meadows [39]. We only consider the excreta produced in a stable for manure supply. We used 90%, the share of the manure for cropland use in developing countries suggested by Smil [59]. Part of the N in animal manure is lost through NH_3 volatilization. Following the assumption from Bouwman et al. [7], 60% of the N in the manure is effective for fertilizer.

2.3. Blue water footprints related to industry and municipal sectors

The data on industrial and domestic water consumption for 1978–1997 are only available in the form of averages over five-year periods. The values for 1978–1982 and 1988–1992 for the YRB were directly available from YRCC [74]; the values for 1983–1987 and 1993–1997 were estimated based on national water withdrawal for industry and household obtained from FAO [19]. In the latter case, we assumed the blue water consumption to be a fraction of blue water withdrawal, taking the fraction equal as the average for the years 1978–1992. Similarly, we assumed the blue water consumption in YRB to be a fraction of the national total equal as the average for the years 1978–1992. For the period 1998–2009, we use annual estimates for industrial and domestic water consumption from YRCC [75].

The blue WFs related to the industrial and municipal sectors in the YRB were downscaled to grid level based on a population density map of the YRB, which was extracted from the 2.5 arc min resolution population density map for China from CIESIN [14]. For downscaling industrial water use, it would have been preferred to use spatial data on industries within the basin, but in absence of such data we used the population density map, following Hoekstra et al. [30]. Monthly industrial and domestic water consumption was obtained by distributing the annual value equally over the 12 months without accounting for the possible variation.

2.4. Blue water scarcity assessment

Blue water scarcity in a catchment is defined as the ratio of the total blue WF ($m^3\ y^{-1}$) to the maximum sustainable blue WF ($m^3\ y^{-1}$) in that catchment during a specific time period [29,30]. In this study, monthly blue water scarcity in the YRB during 1978–2009 was calculated at 5×5 arc min grid. The total blue WF was estimated by summing the crop-related blue WF as calculated in the current study and the blue WFs from the industrial and domestic sectors estimated based on YRCC [75]. The monthly maximum sustainable blue WF was calculated as the 'natural runoff' minus 'environmental flow requirement'. The monthly natural runoff for the study period was obtained from the hydrological model PCR-GLOBWB [65,68,69] at a spatial resolution of 6 × 6 arc min (~9 km × 11 km in the YRB), which was resampled to a resolution of 5 × 5 arc min. The performance of the PCR-GLOBWB for the YRB is good in reproducing variability and magnitudes of monthly natural discharge [65]. The 'environmental flow requirement' was estimated based on the presumptive standard proposed by Richter et al. [52] and Hoekstra et al. [29] and earlier applied by Hoekstra et al. [30]. According to this standard, 80% of monthly natural runoff is allocated to the environment. The maximum sustainable blue WF per grid cell was calculated as 20% of the total natural runoff from that cell and upstream grid cells, minus the blue WF in upstream grid cells.

Blue water scarcity is classified into four levels [30]: 'low' when the blue WF is smaller than 20% of natural runoff, i.e. when the blue WF is smaller than the maximum sustainable blue WF; 'moderate' when the blue WF is between 20% and 30% of natural runoff; 'significant' when the blue WF is between 30% and 40% of natural runoff; and 'severe' when the blue WF exceeds 40% of natural runoff.

Table 2
Share of excretion produced in stables and excretion rates per livestock category.[a]

Livestock	Share of excretion produced in stables (%)	Excretion rate (kg nutrient head^{-1} y^{-1})	
		N	P
Cattle	46	50	10
Goats	10	10	2
Sheep	10	10	2
Pigs	100	12	4
Poultry	100	0.6	0.19

[a] Sources: shares of excretion produced in stables from Bouwman et al. [6] and Liu et al. [39]; excretion rates from Sheldrick et al. [56].

2.5. Data

The GIS polygon data for the YRB and drainage directions at a resolution of 30 × 30 arc s were extracted from HydroSHEDS dataset [37]. For the period 1961–2009, monthly precipitation, ET_0 and temperature data at 30 arc min resolution were extracted from CRU-TS-3.10.01 [26]. Data on irrigated and rain-fed area for each crop at 5 arc min resolution were obtained from Portmann et al. [48]. For crops not available in this database, we used the 5 arc min crop area map from Monfreda et al. [45]. Yearly areas and yields for each crop within the YRB were scaled to fit the yearly agriculture statistics at province level of China obtained from NBSC [46]. For tomatoes, we used estimates of FAOSTAT [20], because NBSC [46] does not contain tomato-specific statistics. The data on crop calendar, maximum root depth and reference harvest index are presented in Table 1. Soil texture data were obtained from ISRIC Soil and Terrain database for China at a 10 km^2 resolution [15]. For hydraulic characteristics for each type of soil, the indicative values provided by AquaCrop were used. Data on total soil water capacity (in %vol) at a spatial resolution of 5 arc min were obtained from Batjes [5].

Annual chemical fertilizer use statistics for China for the study period 1961–2009 were obtained from IFA [32]. Total fertilizer use in the YRB was estimated based on the ratio of the crop area in the YRB to the crop area in China as a whole. Total fertilizer use in the YRB per year was downscaled to crop-specific fertilizer use based on the data on fertilizer use per crop in China as reported by FAO [18]. Livestock density data for the year 2000 were taken from Robinson et al. [53]. The livestock density data for other years were scaled with the yearly national stock statistics for different types of livestock obtained from NBSC [46]. The share of excretion produced in stables was obtained from Bouwman et al. [6] and Liu et al. [39] (Table 2). Following Bouwman et al. [7], it was assumed that 90% of the manure was applied to crop fields and that 60% of the nutrients applied to the field in the form of manure is taken up by the plant. The livestock nutrient excretion rates by type of animal were obtained from the baseline data provided by Sheldrick et al. [56] (Table 2). The values for c_{max} and c_{nat} for the calculation of grey WF were taken from the national surface water quality standard of China [44] (Table 3).

3. Results

3.1. The water footprint of crop production

Over the period 1961–2009, the average annual total green–blue WF of crop production in the YRB was 48.8 × 10^9 $m^3\ y^{-1}$, of which

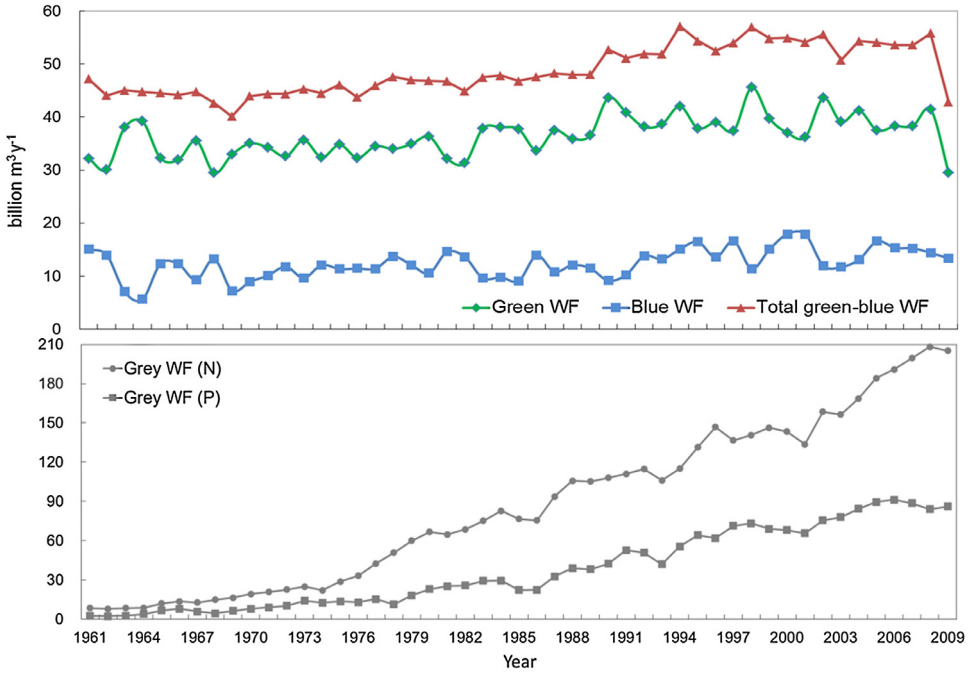

Fig. 1. Annual variability of green, blue and grey water footprints of crop production in the Yellow River Basin. Period: 1961–2009. (For interpretation of the references to colour in this figure legend, the reader is referred to the web version of this article).

Table 3
Water quality parameters for grey water footprint estimation in Yellow River Basin.[a]

Chemical substance	c_{max} (mg l^{-1})	c_{nat} (mg l^{-1})
Phosphorous (P)	0.2	0.02
Nitrogen (N)	1.0	0.2

[a] Source: for c_{nat}, we took data for the best water quality level 'I' in MEP [44].

25% was blue WF (12.4×10^9 m^3 y^{-1}). The average annual grey WF was 86.7×10^9 m^3 y^{-1} related to N and 37.8×10^9 m^3 y^{-1} related to P. The annual variations of green, blue and grey WFs of crop production in the YRB over the study period are plotted in Fig. 1. During the study period, the harvested area of crops considered in the YRB increased little (by about 5%), but the crop production increased by almost five-fold. In order to reach the rising targets for crop production, the irrigated area in the YRB has been expanded 1.5 times relative to the level in the 1960s, which resulted in a 37% larger blue WF in the 2000s (14.4×10^9 m^3 y^{-1}) compared to the 1960s (10.5×10^9 m^3 y^{-1}). The increase in the green WF was less: it was 14% larger in the 2000s (38.4×10^9 m^3 y^{-1}) compared to the 1960s (33.7×10^9 m^3 y^{-1}). As can be seen from Fig. 1, annual green and blue WFs fluctuated inversely, i.e., with an increase in green WF the blue WF decreased. The intensification of crop production and fertilizer application has been one of main reasons for the severe water pollution in the YRB [78]. According to our estimates, the fertilizer-related grey WFs increased over the study period by 24 and 36 times for N and P, respectively. The large increase is not surprising considering the fact that over the period 1961–2009 total fertilizer use on crop land in China increased 38 and 90 times for N and P, respectively [32].

The relative contribution of crops to the total green plus blue WF changed due to changes in cropping patterns in the YRB. In the period 1961–1965, the five biggest contributors to the green plus blue WF related to crop production were winter wheat (48%), spring wheat (8.9%), millet (8.8%), maize (8.3%), and soybean (6.1%), while for 2006–2009 these were winter wheat (41%), maize (21%), spring wheat (7.1%), apples (6.7%) and potatoes (5.2%). Over the study period, crops with increasing green–blue WF of production were winter wheat, rice, maize, potatoes, sunflower, groundnuts, sugar beet, rapeseed, tomatoes and apples. Crops with decreasing green–blue WF were spring wheat, sorghum, millet, barley, soybean, sweet potatoes and cotton (Table 4). Sunflower has the strongest increase in its total WF of production during the study period, which is driven by the huge extension of sunflower planting areas in the YRB (from 1.3 k ha in 1961 to 203 k ha in 2009). Sorghum has the largest decrease in the total WF of production, which relates to the decrease in sorghum planting area by 90%.

In the 2000s, about 62% (8.9×10^9 m^3 y^{-1}) of the crop-related blue WF in the YRB was for wheat production and 21% (3.0×10^9 m^3 y^{-1}) for producing maize. The blue WF of maize production increased nearly five-fold, from 0.65×10^9 m^3 y^{-1} in the 1960s to 3.0×10^9 m^3 y^{-1} in the 2000s. On the other hand, the blue WF of cotton, one of the biggest blue water consumers in the 1960s, dropped from 0.86×10^9 m^3 y^{-1} in the 1960s to 0.63×10^9 m^3 y^{-1} in the 2000s, due to the decline in its irrigated area (~307,000 ha in the 1960s to ~201,000 ha in the 2000s). Regarding the green WF, wheat and maize accounted for about 62% in the 2000s (43% from wheat, 19% from maize). For rapeseed, which is one of the fully rain-fed crops, the green WF share increased from 1% (1960s) to 5% (2000s). Among the crops, maize had the largest grey WF related to both N (60% of the total) and P (48% of the total), followed by soybean (5% of total related to N, 12% of total related to P).

The variation of the total crop-related green–blue WF at basin level is mainly caused by the increase in irrigated area and variation in climatic conditions (like PR and ET_0). The increase of the irrigated area caused the overall increasing trend of the annual blue WF in the YRB, while climate variability contributed to the inter-annual fluctuation of the blue WF. We found that the blue WF decreases with increased PR and increases with increased ET_0, which confirms the finding of Zhuo et al. [80] that the blue WF of crop production is more sensitive to ET_0 than to PR.

The upper, middle and lower reaches accounted for 23%, 49% and 28%, respectively, of the annual average green–blue WF of crop production in the YRB in the 2000s. Over the study period, the increase of the basin's total blue WF mainly happened in the upper reach, while the increase in the total green WF was mainly in the lower

Table 4
Percentage increases in water footprint of crop production in the Yellow River Basin from the period 1961–1970 to the period 2001–2009.

Crop	Increase in total WF (%)				Increase in WF per ton of crop (%)			
	Green	Blue	Grey	Total green–blue	Green	Blue	Grey	Total green–blue
Winter wheat	−1	18	280	4	−77	−73	−12	−76
Spring wheat	−27	25	333	−2	−52	−18	184	−36
Rice	121	167	1320	135	−56	−46	225	−53
Maize	125	362	1890	165	−80	−59	76	−77
Sorghum	−83	−86	1210	−83	−59	−66	3080	−60
Millet	−79	−77	809	−79	−42	−36	2470	−43
Barley	−73	−58	787	−73	−66	−46	1030	−65
Soybean	−37	−40	811	−38	−53	−46	662	−51
Potato	46	196	1590	51	−66	−31	295	−65
Sweet potato	−41	−37	1170	−8	−45	−41	1080	−46
Cotton	−17	−27	634	−20	−64	−69	217	−67
Sugar beet	76	–	3490	76	−63	–	645	−63
Groundnut	266	409	1370	282	−66	−52	37	−64
Sunflower	9110	14900	14100	9630	−44	−8	−13	−41
Rapeseed	385	–	2510	385	−77	–	25	−77
Tomato	251	357	1640	258	−57	−44	113	−56
Apple	1248	1700	2310	1290	−69	−58	−44	−68

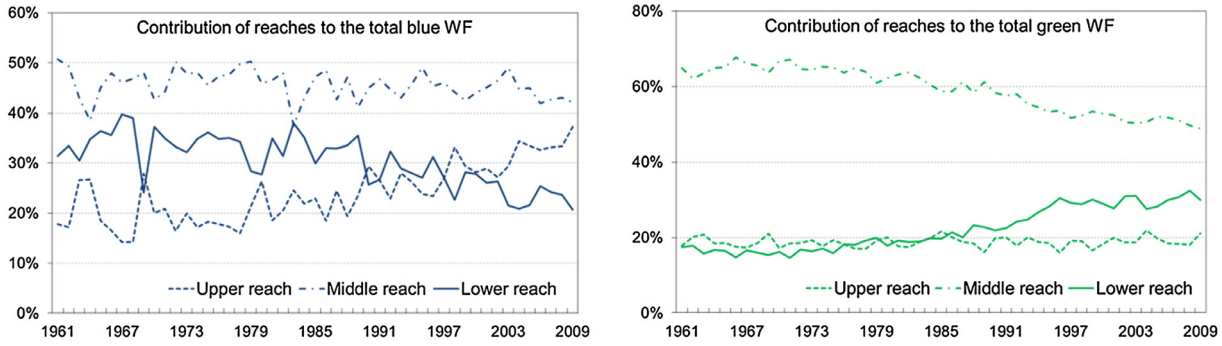

Fig. 2. The relative contribution of the upper, middle and lower reaches to the annual blue (left graph) and green (right graph) water footprints of crop production in the Yellow River Basin. Period: 1961–2009. (For interpretation of the references to colour in this figure legend, the reader is referred to the web version of this article).

reach. Fig. 2 shows the relative contribution of the three reaches to the annual blue and green WFs of crop production in the basin over the period 1961–2009. Over the whole period, the middle reach had the largest share in both the blue and green WF in the basin as a whole, because of its larger share in the basin's total cultivated area (~59% in 2009). With the construction and expansion of main irrigation zones (e.g. Qingtongxia and Hetao irrigation districts) in the arid and semi-arid upper reach, the crop-related WF in this reach as well as the share in the basin total constantly increased and doubled during the five decades. The share of the upper reach in the total blue WF in the YRB reached 37% in 2009. The blue WF in the lower reach fluctuated but remained more or less constant over the study period, although the share in the basin's total blue WF diminished. The green WF in the relatively wet lower reach increased almost two times due to increased cultivation of rain-fed crops such as rapeseed.

The spatial distribution of the total green-blue WF of crops in the YRB (Fig. 3a) follows the distribution of the harvested crop area. The blue share in the total green-blue WF (Fig. 3b) is obviously large in the places where the irrigated areas are most concentrated (Fig. 3c). Also, blue WFs are larger in the drier area of the upper reach (> 60% of the total) than in the semi-arid middle reach and relatively wet lower reach (~40% of the total). The lower reach has high levels of both PR and ET_0. In this region, there is a large potential to improve productivity in rain-fed agriculture. Increased production in the lower reach can contribute to the lessening of the need to produce in the drier regions of the basin and thus to the reduction of irrigation and blue WF in these regions.

3.2. The water footprint per ton of crop

Over the period 1961–2009, the green and blue WF per ton of crop in the YRB reduced significantly, while the grey WF increased. This is shown for the case of cereal crops (wheat, rice, maize, sorghum, millet and barley) in Fig. 4. The average green–blue WF of cereal crops in the YRB decreased from 6540 $m^3\ t^{-1}$ in the 1960s to 1570 $m^3\ t^{-1}$ in the 2000s. The sharp reduction of the green and blue WFs per ton of cereals is a result of the improved crop yields. The land use for crop production within the YRB, adding up to around 10 million hectare for the crops considered in this study, changed little during the five decades studied, but crop production increased by a factor five. Due to the expansion of the irrigated area, the ratio of blue to green WF increased. Meanwhile, the grey WF per ton of cereals rose because of the increasing application rates of artificial fertilizer. Fig. 4 shows how the reduction in consumptive water use (the green plus blue WF) was offset by an increase in degradative water use (the grey WF). The overall grey WF was determined by the N-related grey WF, which was generally bigger than the P-related grey WF. Among the crops studied, the grey WF of sorghum showed the strongest increase (Table 4).

Fig. 5 shows the spatial variation in the green–blue WF per ton of cereal for five different decades. The WF within the YRB reduced from >3000 $m^3\ t^{-1}$ in most areas in the 1960s to about 500–2000 $m^3\ t^{-1}$ in the 2000s. But some regions in the western part of the basin still have low water productivity (large WF per ton). The reason is that there is low precipitation and no or little irrigation in this region (see Fig. 3c), causing high water stress and low crop yields. It is worth noting, though, that there is little cultivation activity in this region. In the

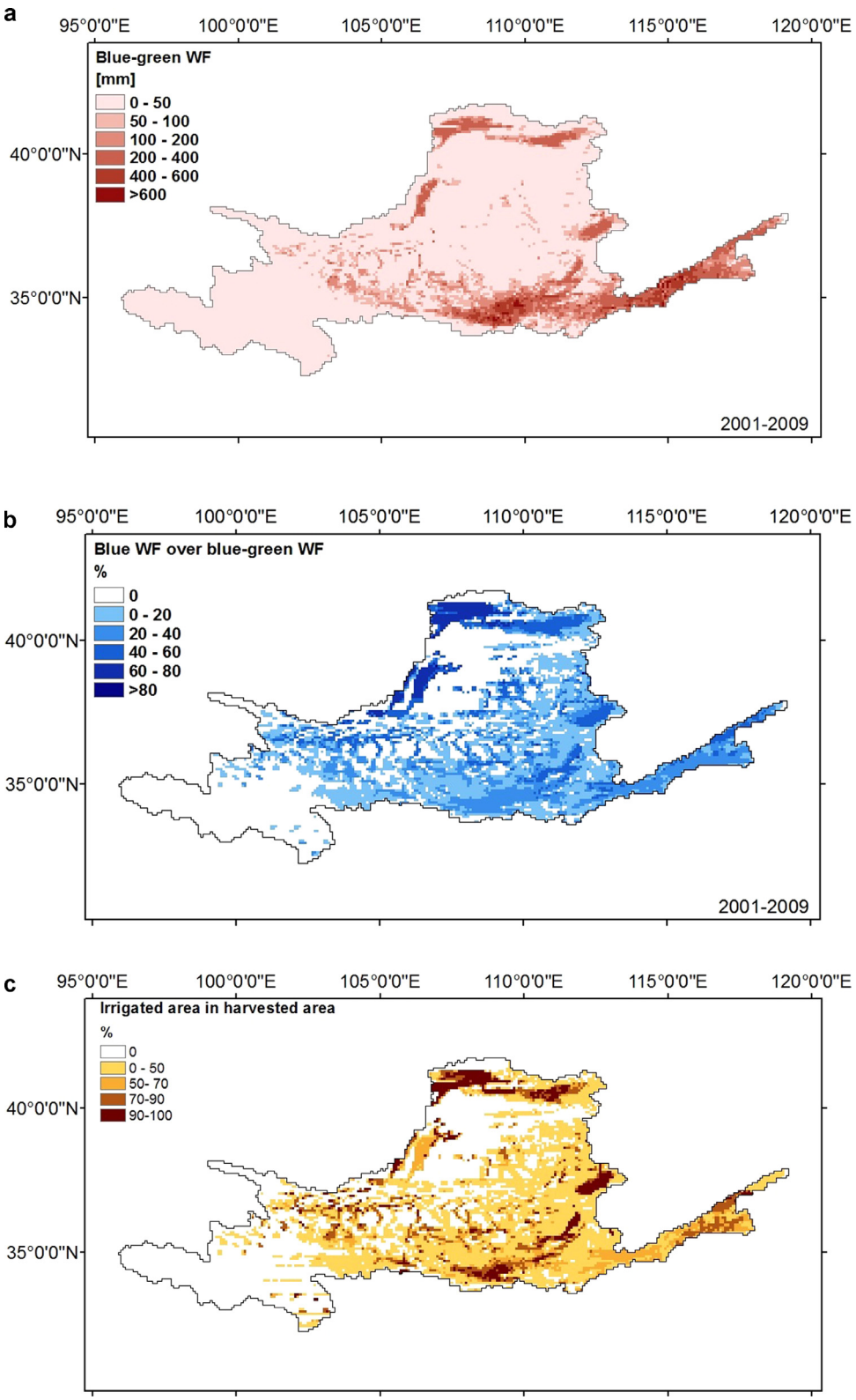

Fig. 3. The spatial distributions of: (a) the average annual green–blue water footprint of crop production (mm), (b) the share of the blue WF in the total green–blue WF (%), and (c) the share of irrigated area in total harvested area (%) in the Yellow River Basin. Period: 2001–2009. (For interpretation of the references to colour in this figure legend, the reader is referred to the web version of this article).

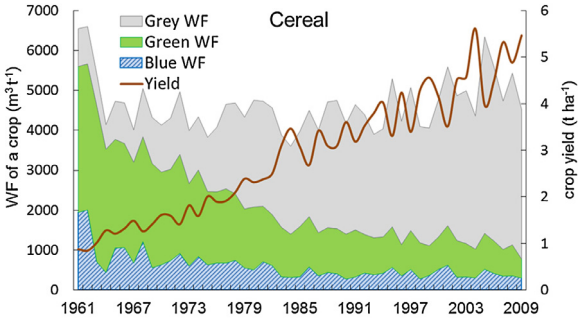

Fig. 4. The green, blue and grey water footprint per ton of cereal ($m^3\ t^{-1}$) and cereal yield ($t\ ha^{-1}$) in the Yellow River Basin. Period: 1961–2009. (For interpretation of the references to colour in this figure legend, the reader is referred to the web version of this article).

2000s, rapeseed had the largest consumptive water use (2678 $m^3\ t^{-1}$) among the crops considered, followed by soybean (2214 $m^3\ t^{-1}$).

3.3. Blue water scarcity within the YRB

The annual blue WF of crop production in the YRB accounts for 73% of the long-term average total blue WF in the basin (including the WF of the industrial and municipal sectors). Blue water scarcity in the YRB during the period 1978–2009 was assessed by comparing the total blue WF from agriculture, industry and households to the maximum sustainable blue WF. According to our estimate, the annual blue WF in the YRB as a whole accounted for 19–52% of the natural runoff, with 31% as the multi-year average, which is higher than the maximum sustainable level (~20% of the natural runoff). Fig. 6 compares, at an annual basis, the total blue WF and the blue WF of crop production alone to the maximum sustainable blue WF and also shows the annual precipitation at the YRB over the study period. The results show that, at yearly scale, relatively large total blue WFs (resulting from additional water demands in agriculture) occur in relatively dry years, when the maximum sustainable blue WF is relatively small, thus enlarging the blue water scarcity.

In order to assess the monthly variability of the blue water scarcity in the YRB, Fig. 7 shows the monthly natural runoff, maximum sustainable blue WF, and blue WF for 1978–2009. The peak of monthly blue WF within a year is asynchronous with the flood season in the basin. The blue WF generally peaks about two months earlier (May–July) than the natural runoff (July–September), which was also observed by [30]. Natural runoff is generally largest from June to October, following the rain season, while the blue WF is largest with the crop growing period from March to July and decreases with higher precipitation after July. As a long-term average, the basin experiences moderate to severe blue water scarcity for seven months per year (January–July), of which on average five months severe (generally March–July).

Fig. 8 zooms in on the monthly blue water scarcity in the YRB for selected wet (2003), dry (2000, 2007) and average (2005) years in the most recent decade of the study period. Monthly blue WF generally peaks in May–July, but the peak in the wet year is much lower than in the average and dry years. Even in the wet year though, the basin experienced moderate to severe blue water scarcity during seven months per year. In the dry year of 2007, there were eleven months in which the blue WF exceeded the maximum sustainable level. Within the study period, the highest value of the monthly blue water scarcity index was 20, observed in April 2000. Although water use for irrigation is the main cause of high blue water scarcity in the YRB, it incidentally happens that moderate to severe blue water scarcity occurs outside the cropping season, in the period November–February, due to the WF of industries and household.

The spatial distributions of monthly blue water scarcity in the YRB in a dry year (2000) and a wet year (2003) are illustrated in Fig. 9 for April (when blue WFs are growing while blue water availability is still low) and July (when both water footprints and blue water availability are high). The eastern part of the upper reach, the northern part of the middle reach, and most of the lower reach suffer severe blue water scarcity throughout the year. In both dry and wet years, about 90% of the basin is likely to face severe blue water scarcity till the start of the flooding season around June. During the last half of the year, the part located in the Tibetan Plateau (western part of the upper reach) has low blue water scarcity because of the absence of irrigation activities and because most of the total basin runoff is generated here. Due to the uneven distribution of the blue WF and available blue water resources across the YRB, about half of the basin still experiences severe blue water scarcity even in the flood season of the wet year even though the blue water scarcity for the basin as a whole is low. This shows the relevance of considering blue water scarcity at a finer spatial scale than river basin level as is usually done.

3.4. Discussion

The current study has been able to assess the inter- and intra-annual variation of the WF of crop production and the blue water scarcity over a few decades at a high spatial resolution in the YRB. Comparing the estimated blue and green WFs in total terms (in $m^3\ y^{-1}$) (averaged for the period 1996–2005) with Mekonnen and Hoekstra [41] shows that the blue WF estimated in the current study agrees better (by 3% lower) to the estimations by Mekonnen and Hoekstra [41] than the green (by 33% lower) and total WF (26% lower). The current total blue WF in the YRB is 4% higher than the assessment by Cai and Rosegrant [8] (for the year 1995). Green–blue WFs per ton of crop were compared with three studies on the YRB [9,41,80] as shown in Fig. 10. Differences are mostly within the range of ±30%,

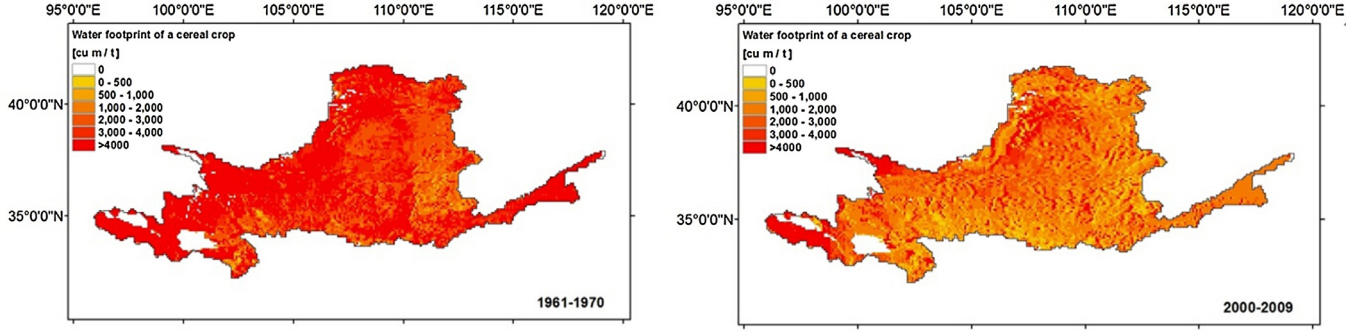

Fig. 5. . Spatial distribution of the decadal average green–blue water footprint ($m^3\ t^{-1}$) of cereal crops in the Yellow River Basin in the period 1961–1970 (left) and 2000–2009 (right). (For interpretation of the references to colour in this figure legend, the reader is referred to the web version of this article).

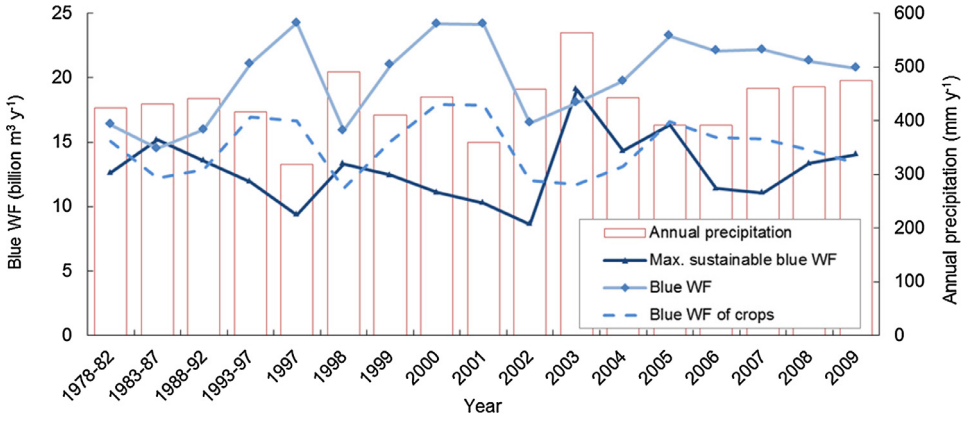

Fig. 6. . The total annual blue water footprint (WF), the annual blue WF of crop production, the maximum sustainable blue WF, and annual precipitation in the Yellow River Basin. Five-year averages for 1978–1997 and year-by-year for 1997–2009. (For interpretation of the references to colour in this figure legend, the reader is referred to the web version of this article).

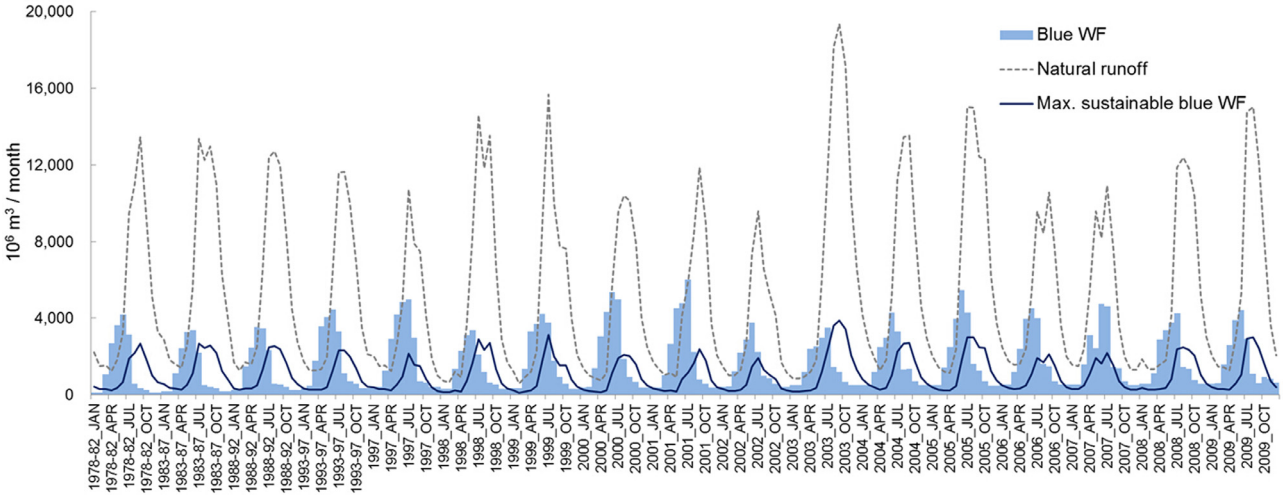

Fig. 7. Monthly blue water footprint (WF) vs. maximum sustainable blue WF and natural runoff within the Yellow River Basin. Five-year averages for 1978–1997 and year-by-year for 1997–2009. (For interpretation of the references to colour in this figure legend, the reader is referred to the web version of this article).

which has been reported as the uncertainty range for WF estimates generated from input uncertainties [80]. Table 5 compares the green, blue and grey WFs of crops in the YRB as estimated in the current study with results from Mekonnen and Hoekstra [41] and Zhuo et al. [80]. The models used and assumptions made in different studies may enhance the level of differences among WF studies. For example, our estimation on the green WF of rapeseed was more than two times the value from Mekonnen and Hoekstra [41], because they calibrated the crop yield at national level while in the current study the calibration was at provincial level, and the rapeseed productivity in the YRB is lower than the national average level. Although we used the same input climate data sources as Zhuo et al. [80], our estimates on the consumptive WF per unit of crop are lower because of the different assumptions on initial soil water content: Zhuo et al. [80] assumed initial soil water content to be at its maximum, i.e. at soil water holding capacity, while in the current study we estimated initial soil water content based on the soil history before planting. The grey WFs of crops presented in the current study are substantially larger than in Mekonnen and Hoekstra [41], which can be explained by the fact that (i) we considered manure fertilizer in the grey WF estimation, which was not considered in Mekonnen and Hoekstra [41] and (ii) we used a stricter assumption on the difference between the maximum allowable and natural N concentration ($c_{max} - c_{nat}$ in Eq. 7), viz. 0.8 mg l^{-1} in the current study versus 10 mg l^{-1} in Mekonnen and Hoekstra [41].

The current study focused on the YRB, but the method used, combining data from climate observations, hydrological models and national statistics, can be applied to other basins as well. Of course, our study is based on a number of limitations. First of all, not all crops were included, although the crops included were responsible for 93% of total crop production in 2009. Also, the WF of forestry and animal husbandry is not included in our simulations. Furthermore, the effects of reservoirs and inter-basin water transfers (the South to North Water Transfer Project) on the temporal and spatial patterns of blue water availability were not considered in the current assessment. Given the fact that blue water withdrawal from reservoirs or transfer projects can make up the blue water shortage in dry months, the maximum sustainable blue WF may have been underestimated and the blue water scarcity over-estimated for some places and months within the basin. However, the presented results on blue water scarcity under natural background conditions, at high spatial and temporal resolution, provide valuable information for improving blue water management (i.e. how to manage reservoirs and water transfer projects to optimally relieve water scarcity). By focussing on blue water scarcity, we excluded an assessment of green water scarcity and the effect of grey WFs on resultant water pollution levels throughout the basin.

Even though based on the most recent insights [52], the assumed environmental flow requirement (80% of natural runoff) may seem too strict and be the reason for the high water scarcity in the basin.

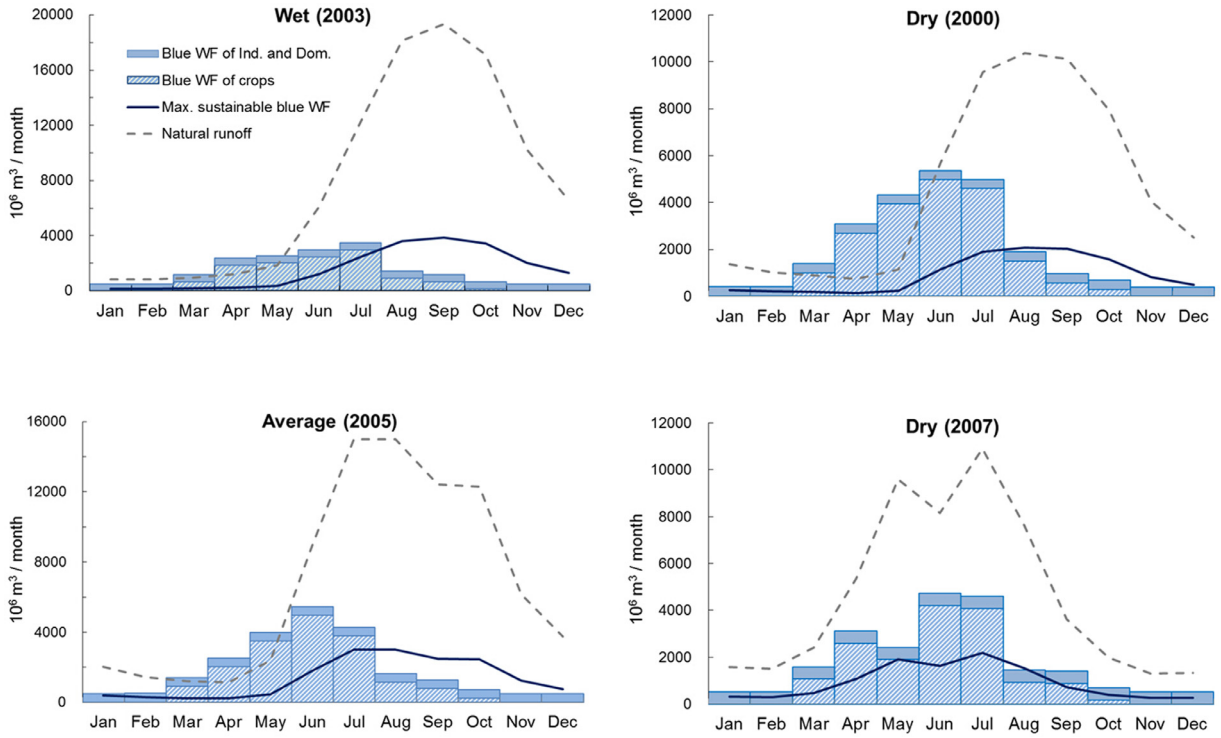

Fig. 8. Monthly blue water footprint (WF) vs. maximum sustainable blue WF and natural runoff within the Yellow River Basin of selected wet (2003), dry (2000, 2007) and average (2005) years. (For interpretation of the references to colour in this figure legend, the reader is referred to the web version of this article).

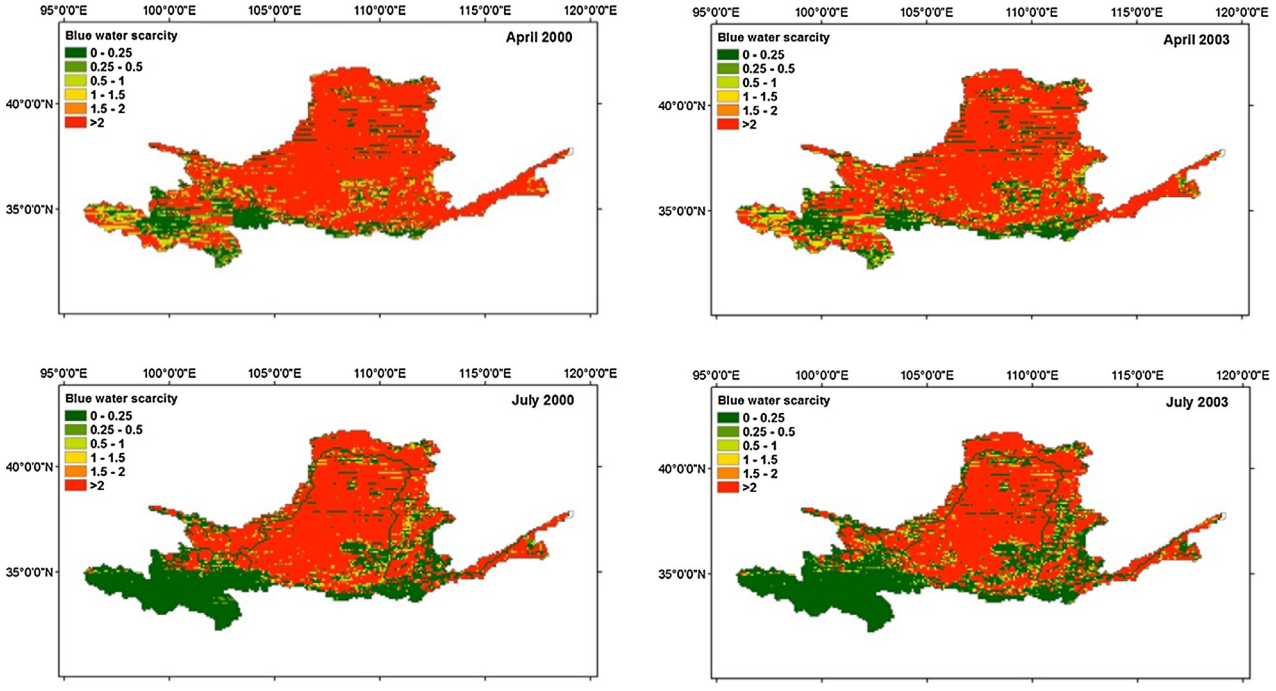

Fig. 9. Monthly blue water scarcity in the Yellow River Basin in the months of April and July in a dry year (2000) and a wet year (2003). (For interpretation of the references to colour in this figure legend, the reader is referred to the web version of this article).

We tested the sensitivity of our water scarcity result by computing scarcity also when assuming an environmental flow requirement of 37% of natural runoff [8,58] or 55% of natural runoff [73]. We found that although the number of months facing moderate to severe blue water scarcity reduced from the current seven months (January–July) to four months (March–June) with the lowest standard (37%), the spatial distribution of blue water scarcity did not change much even in the wettest month in a wet year, with more than half of the basin was still under significant to severe blue water scarcity.

3.5. Conclusion

We assessed the inter-annual variation of WF of crops in the YRB for 1961–2009 with a daily time step, as well as the blue water

Table 5
Comparison between estimated green, blue and grey water footprint of crops in the Yellow River Basin in the current study and previous studies. Period: 1996–2005.

Crop	Green WF (m^3 t^{-1})			Blue WF (m^3 t^{-1})			Grey WF (m^3 t^{-1})	
	Current study	Mekonnen and Hoekstra [41]	Zhuo et al. [80]	Current study	Mekonnen and Hoekstra [41]	Zhuo et al. [80]	Current study	Mekonnen and Hoekstra [41]
Wheat	1241	702	1955	510	532	203	463	313
Rice	414	510	558	225	482	440	5164	215
Maize	542	745	816	195	113	294	7682	293
Sorghum	731	960		45	35		10771	113
Millet	1383	1568		89	30		4993	222
Barley	789	587		61	32		2245	143
Soybean	1626	2370	2130	482	459	163	11075	241
Potato	279	205		15	15		1002	102
Sweet potato	36	257		57	5		1265	64
Cotton	1205	1386		494	343		3366	601
Sugar beet	306	159		0	0		1578	97
Groundnut	1621	1347		296	108		1080	262
Sunflower	1096	2301		145	264		6106	467
Rapeseed	2832	1272		0	0		6617	532
Tomato	198	179		19	5		1631	106
Apple	563	745		72	23		645	286

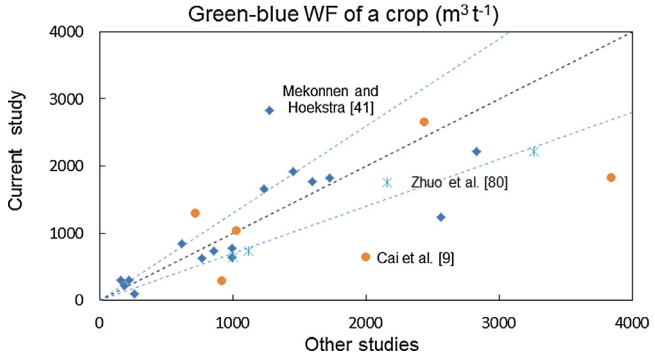

Fig. 10. Comparison of estimated water footprints (WF) of crops with results from previous studies. Each data point refers to the WF of a crop. Period: 1996–2005 for Mekonnen and Hoekstra [41] and Zhuo et al. [80], and 2000–2009 for Cai et al. [9].

scarcity for the period 1978–2009 at monthly basis. The total blue WF of crop production, contributing 25% to the total green–blue WF as a long-term average, increased by 37% from the 1960s till the 2000s, while the green WF grew by 14%. The N- and P-related grey WFs increased by factors of 24 and 36, respectively, along with the increased use of fertilizers. Blue WFs of crop production were larger in years with lower water availability. The increase of the basin's total blue WF in the study period mainly happened in the upper reach, and the share of the upper reach in the basin's total blue WF exceeds the share of the lower reach since 1998. Green and blue WFs of crops per ton reduced significantly (with a factor four for cereal crops) due to improved yields, but the benefits of increased water productivity were completely offset by the five-fold increase in crop production. Related to the expansion of the irrigated area, the proportion of the blue WF in the total green–blue WF increased. Grey WFs per hectare grew quicker than yields, with the net effect that grey WFs per ton of crop increased.

The analysis of blue water scarcity in the YRB showed that the assessment of water scarcity gives more insight when carried out at high spatial resolution level and monthly basis than when done at basin scale and annual basis. But even at basin scale, the annual total blue WF was 19 to 52% of annual natural runoff, and 31% as a long-term average. The annual figures, however, hide the fact that the period with relatively large blue WF (March–July) does not coincide with the period with largest runoff (June–October). On average, the basin faces moderate to severe blue water scarcity during seven months of the year (January–July), of which five months severe (generally March–July). The detailed spatial analysis reveals that the eastern part of the upper reach, the northern part of the middle reach, and most of the lower reach suffer severe blue water scarcity throughout the year. Even in the wettest month in a wet year, about half of the area of the YRB still suffered severe blue water scarcity, especially in the basin's northern part.

Despite the severe water scarcity in the YRB, the Chinese government plans to expand the irrigated cropland area by 12% of the current till the year of 2030 [76]. Therefore the basin is bound to continue facing severe water scarcity in the years to come. Further improvements in crop water productivity will be necessary to prevent aggravation of the water scarcity problem. Water productivities can be improved through increasing yields, reducing non-beneficial evapotranspiration and enhancing effective use of rainfall [42]. Other options include optimizing crop planting dates and choosing crops and varieties that yield more nutritional value per drop of water. Reducing fertilizer use through precision farming will be key in reducing water pollution. In addition, increasing crop imports instead of producing locally within the YRB during dry years will also help saving water [12,36].

Acknowledgments

The work was partially developed within the framework of the Panta Rhei Research Initiative of the International Association of Hydrological Sciences (IAHS). Zhuo is grateful for the scholarship she received from the China Scholarship Council (CSC), No. 2011630181.

References

[1] Abedinpour M, Sarangi A, Rajput T, Singh M, Pathak H, Ahmad T. Performance evaluation of aquacrop model for maize crop in a semi-arid environment. Agricult. Water Manag 2012;110:55–66.
[2] Allen RG, Pereira LS, Raes D, Smith M. Crop evapotranspiration-Guidelines for computing crop water requirements-FAO Irrigation and drainage paper 56, 300. Rome: FAO; 1998. p. D05109.
[3] Andarzian B, Bannayan M, Steduto P, Mazraeh H, Barati M, Barati M, Rahnama A. Validation and testing of the aquacrop model under full and deficit irrigated wheat production in Iran. Agricult. Water Manag 2011;100:1–8.
[4] Araya A, Habtu S, Hadgu KM, Kebede A, Dejene T. Test of aquacrop model in simulating biomass and yield of water deficient and irrigated barley (Hordeum vulgare). Agricult Water Manag 2010;97:1838–46. http://dx.doi.org/10.1016/j.agwat.2010.06.021.
[5] Batjes N. ISRIC-WISE derived soil properties on a 5 by 5 arc-minutes global grid (ver. 1.2). ISRIC; 2012.
[6] Bouwman AF, Lee DS, Asman WAH, Dentener FJ, VanderHoek KW, Olivier JGJ. A global high-resolution emission inventory for ammonia. Global Biogeochem Cy. 1997;11:561–87. http://dx.doi.org/10.1029/97gb02266.

[7] Bouwman L, Goldewijk KK, Van Der Hoek KW, Beusen AHW, Van Vuuren DP, Willems J. Exploring global changes in nitrogen and phosphorus cycles in agriculture induced by livestock production over the 1900–2050 period. P Natl Acad Sci USA 2013;110:20882–7. http://dx.doi.org/10.1073/pnas.1012878108.

[8] Cai X, Rosegrant MW. Optional water development strategies for the yellow river basin: balancing agricultural and ecological water demands. Water Resour Res 2004;40:W08S4.

[9] Cai X, Yang Y-CE, Ringler C, Zhao J, You L. Agricultural water productivity assessment for the yellow river basin. Agricult Water Manag 2011;98:1297–306.

[10] Cai Y, Wang HX, Wang HR, Wang HL. Water footprint in the yellow river basin. J Beijing Normal Univ (Nat Sci) 2009;45:616–20.

[11] Changming L, Shifeng Z. Drying up of the yellow river: its impacts and countermeasures. Mitigation Adapt Strat Global Change. 2002;7:203–14.

[12] Chapagain AK, Hoekstra AY, Savenije HHG. Water saving through international trade of agricultural products. Hydrol Earth Syst Sc. 2006;10:455–68.

[13] Chen Y, Guo G, Wang G, Kang S, Luo H, Zhang D. Main crop water requirement and irrigation of China. Beijing, China: Hydraulic and Electric Press; 1995.

[14] Ciesin C. Gridded population of the world version 3 (GPWV3): population density grids. Palisades, NY: Socioeconomic Data and Applications Center (SEDAC) Columbia University; 2005.

[15] Dijkshoorn K, van Engelen V, Huting J. Soil and landform properties for LADA partner countries. Wageningen, the Netherlands: ISRIC–World Soil Information and FAO; 2008.

[16] Doorenbos J, Kassam A. Yield response to water. Irrigat Drainage Paper. 1979;33:257.

[17] Falkenmark M, Rockström J. Balancing water for humans and nature: the new approach in ecohydrology. Earthscan 2004.

[18] FAO. Fertilizer use statistics. Rome, Italy: Food and Agriculture Organization; 2007.

[19] FAO. AQUASTAT online database. Rome, Italy: Food and Agriculture Organization; 2014.

[20] FAO. FAOSTAT on-line database. Rome, Italy: Food and Agriculture Organization; 2014.

[21] Farahani HJ, Izzi G, Oweis TY. Parameterization and evaluation of the aquacrop model for full and deficit irrigated cotton. Agron J. 2009;101:469–76.

[22] Feng KS, Siu YL, Guan DB, Hubacek K. Assessing regional virtual water flows and water footprints in the yellow river basin, China: a consumption based approach. Appl Geogr. 2012;32:691–701. http://dx.doi.org/10.1016/j.apgeog.2011.08.004.

[23] N. Franke, A. Hoekstra, H. Boyacioglu. Grey water footprint accounting: tier 1 supporting guidelines. (2013).

[24] Garcia-Vila M, Fereres E, Mateos L, Orgaz F, Steduto P. Deficit irrigation optimization of cotton with aquacrop. Agron J. 2009;101:477–87. http://dx.doi.org/10.2134/agronj2008.0179s.

[25] Hanasaki N, Inuzuka T, Kanae S, Oki T. An estimation of global virtual water flow and sources of water withdrawal for major crops and livestock products using a global hydrological model. J Hydrol. 2010;384:232–44. http://dx.doi.org/10.1016/j.jhydrol.2009.09.028.

[26] Harris I, Jones PD, Osborn TJ, Lister DH. Updated high-resolution grids of monthly climatic observations - the CRU TS3.10 Dataset. Int J Climatol. 2014;34:623–42. http://dx.doi.org/10.1002/joc.3711.

[27] Hoekstra A. Virtual water trade: Proceedings of the international expert meeting on virtual water trade. The Netherlands: IHE Delft; 2003.

[28] Hoekstra AY, Chapagain AK. Water footprints of nations: Water use by people as a function of their consumption pattern. Water Resour Manag. 2007;21:35–48. http://dx.doi.org/10.1007/s11269-006-9039-x.

[29] Hoekstra AY, Chapagain AK, Aldaya MM, Mekonnen MM. The water footprint assessment manual: setting the global standard. London, UK: Earthscan; 2011.

[30] Hoekstra AY, Mekonnen MM, Chapagain AK, Mathews RE, Richter BD. Global monthly water scarcity: blue water footprints versus blue water availability. Plos One. 2012:7 ARTN e3268810.1371/journal.pone.0032688.

[31] Hsiao TC, Heng L, Steduto P, Rojas-Lara B, Raes D, Fereres E. Aquacrop-the fao crop model to simulate yield response to water: III. Parameter Testing Maize. Agron J. 2009;101:448–59. http://dx.doi.org/10.2134/agronj2008.0218s.

[32] IFA. IFADATA: IFA statistical databases. International Fertilizer Industry Association; 2013.

[33] Iqbal MA, Shen Y, Stricevic R, Pei H, Sun H, Amiri E, et al. Evaluation of the fao aquacrop model for winter wheat on the North China Plain under deficit irrigation from field experiment to regional yield simulation. Agricult Water Manag 2014;135:61–72.

[34] Jin X, Feng H, Zhu X, Li Z, Song S, Hui D. Assessment of the aquacrop model for use in simulation of irrigated winter wheat canopy cover, biomass, and grain yield in the North China plain. Plos One. 2014;9:e86938.

[35] Katerji N, Campi P, Mastrorilli M. Productivity, evapotranspiration, and water use efficiency of corn and tomato crops simulated by AquaCrop under contrasting water stress conditions in the Mediterranean region. Agricult Water Manag 2013;130:14–26.

[36] Konar M, Dalin C, Suweis S, Hanasaki N, Rinaldo A, Rodriguez-Iturbe I. Water for food: the global virtual water trade network. Water Resources Res 2011;47.

[37] Lehner B, Verdin K, Jarvis A. New global hydrography derived from spaceborne elevation data. EOS, Trans Amer Geophys Union 2008;89:93–4.

[38] Liu JG, Yang H. Spatially explicit assessment of global consumptive water uses in cropland: green and blue water. J Hydrol. 2010;384:187–97. http://dx.doi.org/10.1016/j.jhydrol.2009.11.024.

[39] Liu JG, You LZ, Amini M, Obersteiner M, Herrero M, Zehnder AJB, Yang H. A high-resolution assessment on global nitrogen flows in cropland. P Natl Acad Sci USA 2010;107:8035–40. http://dx.doi.org/10.1073/pnas.0913658107.

[40] Liu Q, McVicar TR. Assessing climate change induced modification of Penman potential evaporation and runoff sensitivity in a large water-limited basin. J Hydrol. 2012;464:352–62.

[41] Mekonnen MM, Hoekstra AY. The green, blue and grey water footprint of crops and derived crop products. Hydrol Earth Syst Sc. 2011;15:1577–600. http://dx.doi.org/10.5194/hess-15-1577-2011.

[42] Mekonnen MM, Hoekstra AY. Water footprint benchmarks for crop production: a first global assessment. Ecol Indic. 2014;46:214–23. http://dx.doi.org/10.1016/j.ecolind.2014.06.013.

[43] Mekonnen MM, Hoekstra AY. Global grey water footprint and water pollution levels related to anthropogenic nitrogen loads to fresh water. Environ Sci Technol. 2015. http://dx.doi.org/10.1021/acs.est.5b03191.

[44] MEP. Surface water quality standards in China (GB3838-2002). Beijing, China: Ministry of Environmental Protection; 2002.

[45] Monfreda C, Ramankutty N, Foley JA. Farming the planet: 2. Geographic distribution of crop areas, yields, physiological types, and net primary production in the year 2000. Global Biogeochem Cy. 2008;22 Artn Gb1022. http://dx.doi.org/10.1029/2007gb002947.

[46] NBSC. National data. in: NBoSo China, (Ed.). NBSC 2013.

[47] Perry C. Efficient irrigation; inefficient communication; flawed recommendations. Irrigat Drainage. 2007;56:367–78.

[48] Portmann FT, Siebert S, Doll P. MIRCA2000-Global monthly irrigated and rainfed crop areas around the year 2000: a new high-resolution data set for agricultural and hydrological modeling. Global Biogeochem Cy. 2010;24 Artn Gb1011. http://dx.doi.org/10.1029/2008gb003435.

[49] Raes D, Steduto P, Hsiao TC, Fereres E. Aquacrop-the fao crop model to simulate yield response to water: II. Main Algorith Software Description. Agron J. 2009;101:438–47. http://dx.doi.org/10.2134/agronj2008.0140s.

[50] Raes D, Steduto P, Hsiao TC, Fereres E. Reference manual AquaCrop version 4.0. Food and Agriculture Organization, Rome, Italy; 2011.

[51] Rallison RE. Origin and evolution of the SCS runoff equation. Symposium on Watershed Management 1980. ASCE; 1980. p. 912–24.

[52] Richter BD, Davis M, Apse C, Konrad C. A presumptive standard for environmental flow protection. River Res Appl 2012;28:1312–21.

[53] Robinson TP, Franceschini G, Wint W. The food and agriculture organization's gridded livestock of the world. Vet Ital. 2007;43:745–51.

[54] Rost S, Gerten D, Bondeau A, Lucht W, Rohwer J, Schaphoff S. Agricultural green and blue water consumption and its influence on the global water system. Water Resources Res 2008;44.

[55] Savenije H. Water scarcity indicators; the deception of the numbers. Phys Chem Earth, Part B: Hydrol Oceans Atmos 2000;25:199–204.

[56] Sheldrick W, Syers JK, Lingard J. Contribution of livestock excreta to nutrient balances. Nutrient Cyc Agroecosyst 2003;66:119–31.

[57] Siebert S, Doll P. Quantifying blue and green virtual water contents in global crop production as well as potential production losses without irrigation. J Hydrol. 2010;384:198–217. http://dx.doi.org/10.1016/j.jhydro1.2009.07.031.

[58] Smakhtin V, Revenga C, Döll P. A pilot global assessment of environmental water requirements and scarcity. Water Int. 2004;29:307–17.

[59] Smil V. Nitrogen in crop production: an account of global flows. Global Biogeochem Cy. 1999;13:647–62. http://dx.doi.org/10.1029/1999gb900015.

[60] Steduto P, Hsiao TC, Fereres E. On the conservative behavior of biomass water productivity. Irrigation Sci 2007;25:189–207.

[61] Steduto P, Hsiao TC, Raes D, Fereres E. Aquacrop-the fao crop model to simulate yield response to water: I. Concepts Underlying Principles. Agron J. 2009;101:426–37. http://dx.doi.org/10.2134/agronj2008.0139s.

[62] Stricevic R, Cosic M, Djurovic N, Pejic B, Maksimovic L. Assessment of the FAO AquaCrop model in the simulation of rainfed and supplementally irrigated maize, sugar beet and sunflower. Agricult Water Manag 2011;98:1615–21.

[63] Sun SK, Wu PT, Wang YB, Zhao XN, Liu J, Zhang XH. The temporal and spatial variability of water footprint of grain: a case study of an irrigation district in China from 1960 to 2008. J Food Agric Environ. 2012;10:1246–51.

[64] Tuninetti M, Tamea S, D'Odorico P, Laio F, Ridolfi L. Global sensitivity of high-resolution estimates of crop water footprint. Water Resour Res 2015.

[65] Van Beek L, Wada Y, Bierkens MF. Global monthly water stress: 1. Water balance and water availability. Water Resources Res 2011;47.

[66] Vanuytrecht E, Raes D, Willems P. Global sensitivity analysis of yield output from the water productivity model. Environ Model Software 2014;51:323–32.

[67] Vörösmarty CJ, McIntyre PB, Gessner MO, Dudgeon D, Prusevich A, Green P, et al. Global threats to human water security and river biodiversity. Nature. 2010;467:555–61. http://dx.doi.org/10.1038/nature09440.

[68] Wada Y, Bierkens MFP. Sustainability of global water use: past reconstruction and future projections. Environ Res Lett 2014;9 Artn 104003. http://dx.doi.org/10.1088/1748-9326/9/10/104003.

[69] Wada Y, Van Beek L, Viviroli D, Dürr HH, Weingartner R, Bierkens MF. Global monthly water stress: 2. Water demand and severity of water stress. Water Resources Res 2011:47.

[70] Xie G, Han D, Wang X, Lü R. Harvest index and residue factor of cereal crops in China. J China Agricult Univ 2011;16:1–8.

[71] Xu K, Milliman JD, Xu H. Temporal trend of precipitation and runoff in major Chinese Rivers since 1951. Global Planet Change 2010;73:219–32.

[72] Xu Z, Li J, Liu C. Long-term trend analysis for major climate variables in the yellow river basin*. Hydrol Proc 2007;21:1935–48.

[73] Yang Z, Sun T, Cui B, Chen B, Chen G. Environmental flow requirements for integrated water resources allocation in the yellow river basin, China. Commun Nonlin Sci Numer Simul 2009;14:2469–81.

[74] YRCC. Water use and planning. Zhengzhou, China: Yellow River Conservancy Commission; 2006.
[75] YRCC. Yellow River water resource bulletin 1998-2009. Zhengzhou, China: Yellow River Conservancy Commission; 2011.
[76] YRCC. Comprehensive planning of the Yellow River Basin for 2012-2030. Zhengzhou, China: Yellow River Conservancy Commission; 2013.
[77] Yuan M, Zhang L, Gou F, Su Z, Spiertz J, van der Werf W. Assessment of crop growth and water productivity for five C 3 species in semi-arid Inner Mongolia. Agricult Water Manag 2013;122:28–38.
[78] Yunpeng X, Sun Y, Ringler C. Governance, Laws, and Water Interventions in the Yellow River Basin Over the Past 60 Years: From Supply-to Demand-Side Management, International Food Policy Research Institute, Washington, D. C., USA; 2015.
[79] Zhang F, Zhu Z. Harvest index for various crops in China. Scientia Agricultura Sinica. 1990;23:83–7.
[80] Zhuo L, Mekonnen M, Hoekstra A. Sensitivity and uncertainty in crop water footprint accounting: a case study for the yellow river basin. Hydrol Earth Syst Sc. 2014;18:2219–34.